

# Nonlinear Control of Chaotic Systems: A Switching Manifold Approach

JIN-QING FANG<sup>a,\*</sup>, YIGUANG HONG<sup>b</sup>, HUASHU QIN<sup>b</sup> and GUANRONG CHEN<sup>c</sup>

<sup>a</sup>China Institute of Atomic Energy, P.O. Box 275-27, Beijing 102413, P.R. China; <sup>b</sup>Institute of Systems Science, Academia Sinica, Beijing 100080, P.R. China; <sup>c</sup>Department of Electrical and Computer Engineering, University of Houston, Houston, TX 77204-4793, USA

(Received 20 November 1998)

**In this paper, a switching manifold approach is developed for nonlinear feed-back control of chaotic systems. The design strategy is straightforward, and the nonlinear control law is the simple bang–bang control. Yet, this control method is very effective; for instance, several desired equilibria can be stabilized by using one control law with different initial conditions. Its effectiveness is verified by both theoretical analysis and numerical simulations. The Lorenz system simulation is shown for the purpose of illustration.**

*Keywords:* Chaos control, Nonlinear control, Switching manifold approach, Lorenz chaotic system

*PACS:* 05.45 + b, 89.70 + c, 43.72 + q, 47.52 + j

## INTRODUCTION

In recent years, chaos control has received increasing attention from the communities of physics, engineering, mathematics, and biomedical sciences, due to its great potential applications in many interdisciplinary areas such as laser and plasma physics, secure signal and image communications, human heart and brain signal analyses, chemical reactions, power electronics, and fluid dynamics as well as economics and ecology [1–6].

Although significant progress has been achieved, profound theories, deep understanding and unified methodologies for chaos control are still in their forming and developing phase.

Most existing methods for controlling chaos are based on linear or linearized controls, which are often not satisfactory since it is not always possible to use a linear controller to well handle a nonlinear system, particularly a complex chaotic system. On many occasions, nonlinear control methods prove to be necessary. In fact, nonlinear controls are

---

\* Corresponding author.

promising not only for chaotic systems but also for various types of nonlinear and complex dynamical processes.

There have been some nonlinear feedback control methods developed for chaos control [3–10]; some of them have been extended to controlling hyperchaos as well as spatiotemporal chaos [11–12]. A basic reason is that nonlinear control is generally superior over linear ones, especially when the objective is to have optimal control performance, such as achieving the fastest control time, the desired transient response, or some specified robustness properties. One typical method is the variable structure control, known also as sliding mode control, which has the advantage of being robust to system parameter variation and external perturbation. In this approach, the controller follows a switching law that can guide the system trajectory to a stable manifold (called the switching manifold), as demonstrated for the Lorenz system in [13,14]. Here, it is noted that when these variable structure control methods are applied, different switching manifolds and control laws are generally needed if the system orbits are controlled to different equilibria. As another reference, this type of strategy was used for control and synchronization of discrete-time chaotic systems [15], where input–output linearization remains to be the main methodology.

In this paper, we present two switching manifold and nonlinear feedback methods for controlling chaos. The design strategy is simple, and the nonlinear control law is a bang–bang control. This method differs from those of [13–15] in that this approach only needs one control law to stabilize several desired unstable equilibria, by changing either the initial condition or the feedback control gain.

## 1. THE CHAOS CONTROL PROBLEM AND DESIGN PRINCIPLE

Consider an  $n$ -dimensional chaotic system,

$$\dot{x} = F(x), \quad x \in R^n. \quad (1.1)$$

To stabilize a desired unstable equilibrium embedded in the chaotic attractor, a controller is applied:

$$\dot{x} = F(x) + G(x)u, \quad u \in R^m, \quad (1.2)$$

where  $G(x)$  is an  $n \times m$  matrix-valued nonlinear function to be determined alongside of the controller  $u(\cdot)$ .

To design a nonlinear controller for the intended task, the basic principle is summarized as follows. To start, a switching manifold, which containing the target equilibrium, is first identified. Then, using a bang–bang control, the system state is driven from outside the manifold (usually nearby) to move toward the manifold. In much the same way, the other switching manifold is obtained for another equilibrium and the system state near the target is forced to slide onto it. The control law so designed is in a simple nonlinear feedback form. Details are illustrated in the following sections.

## 2. ANALYSIS OF THE SWITCHING MANIFOLD STRATEGY

To clarify the basic idea, let us consider the well-known controlled Lorenz equation as a typical example, which is described by

$$\begin{cases} \dot{x}_1 = -\sigma(x_1 - x_2) + u \\ \dot{x}_2 = \rho x_1 - x_2 - x_1 x_3 \\ \dot{x}_3 = x_1 x_2 - b x_3 \end{cases} \quad (2.1)$$

where, corresponding to (1.2),

$$\begin{cases} F(x) = (-\sigma(x_1 - x_2), \\ \rho x_1 - x_2 - x_1 x_3, x_1 x_2 - b x_3)^\top \\ G(x) = (1, 0, 0)^\top. \end{cases}$$

To obtain an effective control law, we use the feedback in the form of

$$|u| \leq \epsilon \quad (2.2)$$

or

$$u = u_{\text{eq}} + u_0, \quad |u_0| \leq \epsilon \quad (2.3)$$

where  $\epsilon$  is an upper bound specified by physical and/or engineering limitations, and  $u_{\text{eq}}$  is a control law to be designed later.

The Lorenz system has a chaotic attractor for the parameters  $\sigma = 10$ ,  $b = 8/3$ , and  $\rho = 28$ . According to the analysis of local stability of the Lorenz system, there are two unstable equilibria in the attractor:

$$P = (\sqrt{b(\rho - 1)}, \sqrt{b(\rho - 1)}, \rho - 1)^\top \quad \text{and} \\ Q = (-\sqrt{b(\rho - 1)}, -\sqrt{b(\rho - 1)}, \rho - 1)^\top.$$

Our goal is to find a state-feedback controller, in the form of (2.2) or (2.3), to stabilize the system and to arrive at the equilibrium  $P$  or  $Q$ , using the right initial condition and a suitable feedback control gain.

To do so, a switching manifold,

$$s = s(x) \quad (2.4)$$

is first identical, such that:

- (i) it contains all targets, namely,  $P$  and  $Q$ ;
- (ii) it is transversal to the column vectors of the input matrix,  $G(x)$ , almost everywhere near  $P$  and  $Q$ , namely, its tangential vector near  $P$  and  $Q$  is not parallel to the column vectors of  $G(x)$ ;
- (iii) it is a locally stable manifold around the targets  $P$  and  $Q$ ; that is, within the manifold  $s(x) = 0$  both  $P$  and  $Q$  are stable equilibria.

For system (2.1), the manifold can be taken in the following form (which is not unique):

$$s(x) = bx_3 - x_1^2 = 0. \quad (2.5)$$

It is easy to see that the first and second conditions can be satisfied by this switching manifold, namely, the two points  $P$  and  $Q$  are located in the manifold and the vector  $G(x) = (1, 0, 0)^\top$  is transversal to the manifold around these two points. Notice,

moreover, that

$$\dot{s} = b(x_1x_2 - bx_3) - 2x_1(-\sigma(x_1 - x_2) + u) \quad (2.6)$$

so that

$$\frac{\partial \dot{s}}{\partial u} = -2x_1 \quad (2.7)$$

which does not vanish in the manifold (2.5) except at the point  $x_1 = 0$ . This means, when  $x_1 \neq 0$ ,  $\dot{s}$  can be controlled directly by  $u$ . Therefore,  $u$  can be so chosen to force  $s \rightarrow 0$ .

As to the third condition, we only verify the stability around the point  $P$  on the manifold, since the analysis for the point  $Q$  is similar. In system (2.1), we first shift the point  $P$  to the origin, by using the transformation

$$z_1 = x_1 - \sqrt{b(\rho - 1)}, \\ z_2 = x_2 - \sqrt{b(\rho - 1)}, \\ z_3 = x_3 - \rho + 1$$

which yields

$$\begin{cases} \dot{z}_1 = -\sigma(z_1 - z_2) \\ \dot{z}_2 = z_1 - z_2 - z_1z_3 - \sqrt{b(\rho - 1)}z_3 \\ \dot{z}_3 = z_1z_2 + \sqrt{b(\rho - 1)}(z_1 + z_2) - bz_3. \end{cases} \quad (2.8)$$

Consequently, the manifold (2.5) becomes

$$s(z) = bz_3 - z_1^2 - 2\sqrt{b(\rho - 1)}z_1 = 0 \quad (2.9)$$

which gives

$$z_3 = \frac{1}{b}z_1(z_1 + 2\sqrt{b(\rho - 1)}).$$

Substituting it into system (2.8) yields the reduced dynamics on manifold (2.10); that is,

$$\begin{cases} \dot{z}_1 = -\sigma(z_1 - z_2) \\ \dot{z}_2 = (3 - 2\rho)z_1 - z_2 - \frac{1}{b}z_1[z_1^2 + 3\sqrt{b(\rho - 1)}z_1]. \end{cases} \quad (2.10)$$

Because the linear approximation of system (2.10), after dropping the higher-order terms, is

$$\begin{cases} \dot{z}_1 = -\sigma(z_1 - z_2) \\ \dot{z}_2 = (3 - 2\rho)z_1 - z_2 \end{cases}$$

which is asymptotically stable at  $(z_1, z_2) = (0, 0)$ , system (2.10) is (locally) asymptotically stable near the point  $P$ .

In much the same way, the point  $Q$  can be shifted to a new, locally stable equilibrium.

*Remark 1* Another equilibrium,  $x = (x_1, x_2, x_3) = (0, 0, 0)$ , is also in the manifold (2.5) and the dynamics on this manifold near the point  $x = 0$  can also be derived. In fact, its behavior is just like a saddle point on (2.5). For this point, the switching manifold cannot be used to stabilize it since it is not even locally stable in the manifold.

*Remark 2* If  $G(x)$  is taken as  $[0, 1, 0]^\top$ , then the controlled Lorenz system becomes

$$\begin{cases} \dot{x}_1 = -\sigma(x_1 - x_2) \\ \dot{x}_2 = \rho x_1 - x_2 - x_1 x_3 + u \\ \dot{x}_3 = x_1 x_2 - b x_3 \end{cases} \quad (2.11)$$

As symmetrical to the above result, a selected switching manifold for the current case is

$$s(x) = b x_3 - x_2^2 = 0 \quad (2.12)$$

which, again, is not a unique choice. Actually, the manifolds (2.5) and (2.12) can both be used successfully for controlling the Lorenz system, as shown in our numerical simulations below.

### 3. NONLINEAR FEEDBACKS

In the last section, two possible switching manifolds (2.5) and (2.12), are formulated and the reduced system dynamics on these manifolds were analyzed. Now, we are in a position to design a suitable controller to guide the system nearby states to converge to the selected manifold.

Observe that the task of control is simply to force  $s \rightarrow 0$ . Therefore, consider Eq. (2.6) again, namely,

$$\dot{s} = b(x_1 x_2 - b x_3) - 2x_1 u + 2\sigma x_1(x_1 - x_2). \quad (3.1)$$

If all the variables,  $x_1, x_2, x_3$ , can be measured directly, the control law can be chosen to be in the form of (2.3), that is,

$$u = u_{\text{eq}} + u_0, \quad (3.2)$$

where  $u_{\text{eq}}$  is determined such that  $\dot{s} = 0$  when  $s = 0$ . Physically,  $u_{\text{eq}}$  plays a role of supplement control when drift error occurs due to the control of  $u_0$ , as can be seen from the numerical simulations discussed below.

It follows from Eq. (2.5) that

$$-b^2 x_3 = -bs - b x_1^2$$

so that Eq. (3.1) can be rewritten as

$$\dot{s} = b x_1 x_2 - bs - b x_1^2 + 2\sigma x_1(x_1 - x_2) - 2x_1 u.$$

Then, it is easy to derive that

$$u_{\text{eq}} = (\sigma - b/2)(x_1 - x_2). \quad (3.3)$$

On the other hand, we may set  $u_0 = \epsilon \operatorname{sgn}[x_1 s]$ , that is, when  $x_1 s > 0$ ,  $u_0 = \epsilon$ ; when  $x_1 s < 0$ ,  $u_0 = -\epsilon$ ; and when  $x_1 s = 0$ ,  $u_0 = 0$ .

In this way, Eq. (3.1), along with the feedback (3.2), leads to a stable manifold,

$$\dot{s} = -bs - \epsilon x_1 \operatorname{sgn}[x_1 s]. \quad (3.4)$$

*Remark 3* When  $u_0$  is taken to be 0 in (3.2),  $\epsilon = 0$ , but manifold (3.4) is still stable. However, with  $u_0 \neq 0$ , Eq. (3.4) has a positive  $\epsilon$ , the convergent rate may be greatly improved.

In many practical situations, some of the state variables of  $x$  cannot be directly measured. For example, if  $x_2$  cannot be used directly in the feedback controller, a nonlinear feedback may be adopted in the form

$$u = \epsilon \operatorname{sgn}[x_1 s]$$

or

$$u = (\sigma - b/2)(x_1 - x_2) + \epsilon \operatorname{sgn}[x_1 s].$$

The strategy is as follows. When  $s > 0$ , we should ensure  $\dot{s} < 0$ . In doing so, there are three cases:

- (1) if  $x_1 > 0$ , let  $u = \epsilon > 0$ ;
- (2) if  $x_1 < 0$ , let  $u = -\epsilon < 0$ ;
- (3) if  $x_1 = 0$ , then (3.1) becomes  $\dot{s} = -b^2 x_3$ ; it follows from  $s > 0$  and  $x_1 = 0$  that  $x_3 > 0$ ; therefore,  $\dot{s} < 0$  in this case.

When  $s < 0$ , to ensure  $\dot{s} < 0$ , the control can be obtained in three cases:

- (4) if  $x_1 > 0$ , let  $u = -\epsilon < 0$ ;
- (5) if  $x_1 < 0$ , let  $u = \epsilon > 0$ ;
- (6) if  $x_1 = 0$ , similar to case (3) above,  $\dot{s} < 0$ .

All cases considered, the control law in the form of (2.2) is obtained as

$$u = u_0 = \epsilon \operatorname{sgn}[x_1(bx_3 - x_1^2)]. \quad (3.5)$$

*Remark 4* Equation (3.5) is limited by its gain and less dependent on the measured variables. So, this controller is practical, though it will be more difficult than the controller in the form of (2.3) when theoretical analysis is performed. In fact, this kind of control laws usually stabilize the system trajectory only to a point near the target equilibrium, but not necessarily the intended one. Nevertheless, similar to the OGY method and some other techniques based on the ergodic properties of chaos [1–4], the control law here may be added to system (2.1) (or (2.11)) only when a system state is moving to be close to manifold (2.5) (or (2.12)).

*Remark 5* In the case of (2.12), the controls in the forms of (2.2) and (2.3) can also be chosen as follows:

$$u = u_0 = \epsilon \operatorname{sgn}[x_2(bx_3 - x_2^2)] \quad (3.6)$$

or

$$u = x_1[x_3 - (\rho - b/2)] + (1 - b/2)x_2 + \epsilon \operatorname{sgn}[x_2(bx_3 - x_2^2)]. \quad (3.7)$$

These controllers are also effective, as demonstrated by numerical simulation results blow.

*Remark 6* It is worth mentioning that the above ideas can be applied to chaos synchronization as well. For example, consider the case of synchronizing two Lorenz systems in which the state of one system is denoted by  $x$  and the other, by  $y$ . Set the error variable  $e = x - y$  and modify the above nonlinear control methods (or find a new switching error manifold). Then the chaotic synchronization can be realized via control. This topic will be investigated in more detail elsewhere.

#### 4. SIMULATION AND DISCUSSION

To demonstrate the above theoretical analysis, we have studied various numerical simulations for the controlled Lorenz system (2.1) and (2.11), respectively.

Figures 1 and 2 show the projections of stabilized equilibria of Eq. (2.1), controlled by (3.5) in the form of (2.2), and by (3.3) and (3.5) in the form of (2.3), respectively. Both figures were produced under the same initial condition  $x(0) = (0, 2, 7)^\top$  and feedback gain  $\epsilon = 4.5$ .

Figure 1(a) shows the projection of the original Lorenz attractor in the  $x_3$ - $x_1$  plane without any control (for comparison purpose). It is seen from Fig. 1(b) and (c) that the stabilized equilibrium  $Q' = (-8.54, -8.54, 27.39)^\top$  is close to the original target equilibrium,  $Q = (-8.485, -8.485, 27.000)^\top$ , of the Lorenz attractor. In other words, the controller  $u_0 = \epsilon \operatorname{sgn}[x_1(bx_3 - x_1^2)]$  cannot stabilize the system state to the intended equilibrium  $Q$  (or  $P$ ). However, when using the controller (2.3), namely  $u = u_0 + u_{\text{eq}} = \epsilon \operatorname{sgn}[x_1(bx_3 - x_1^2)] + (\sigma - b/2)(x_1 - x_2)$ , even with the same gain value  $\epsilon = 4.5$  and initial condition, system (2.1) can be stabilized exactly to the target equilibrium  $P = (8.485, 8.485, 27.000)^\top$  in the desired precision.

Many other numerical simulations have also verified that the above theoretical analysis is correct, that is, only using  $u_0$  does not always accomplish precise control to the desired target since

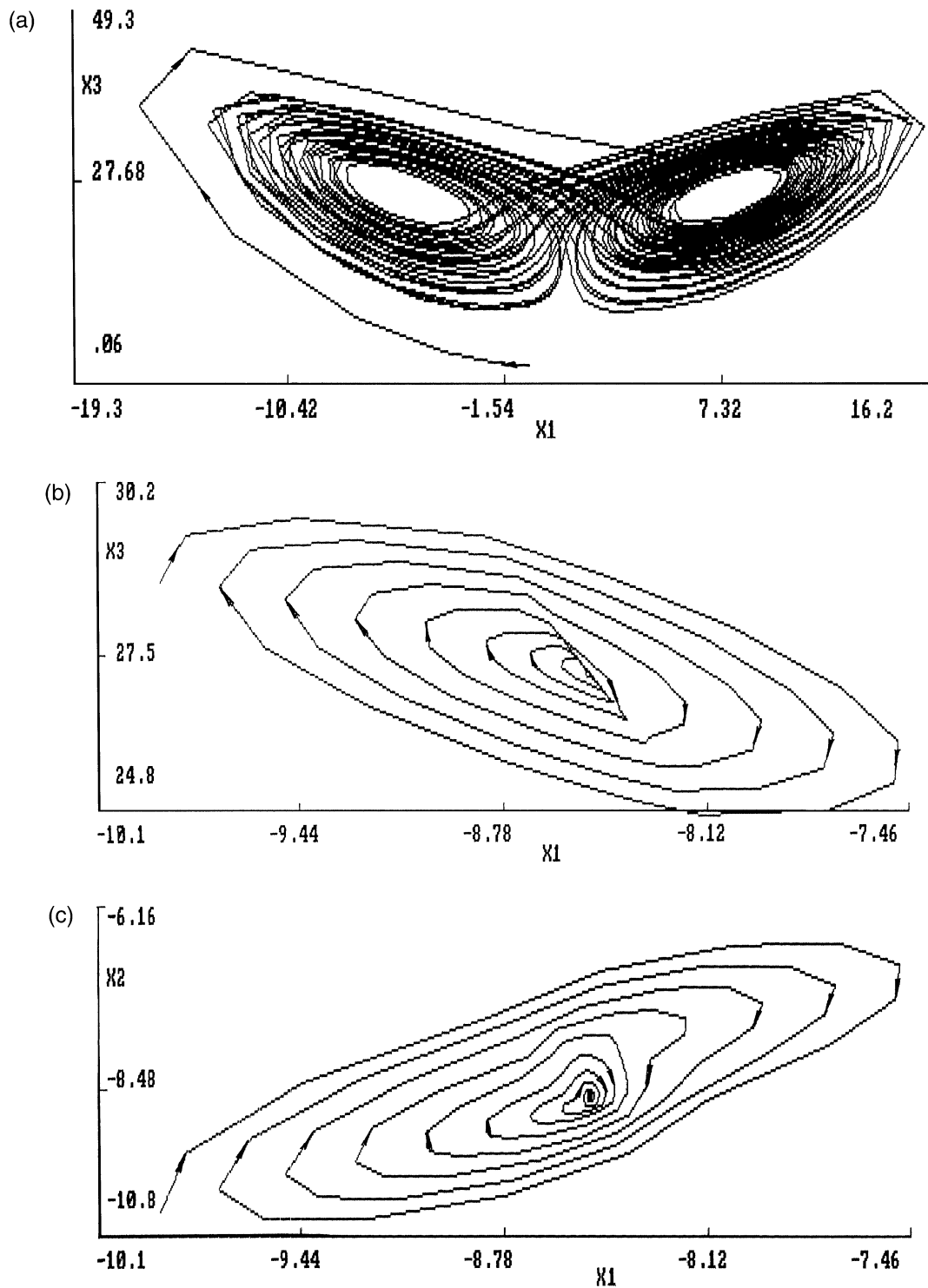


FIGURE 1 Comparison of the Lorenz attractor without control and with control, both with  $x(0) = (0, 2, 7)^T$  and  $\epsilon = 4.5$   
 (a) Projection in the  $x_3-x_1$  plane, without control. (b) Projection in the  $x_3-x_1$  plane, in which the stabilized equilibrium is  $Q' = (-8.54, -8.54, 27.39)^T$  of the Lorenz attractor controlled by (3.5) in the form of (2.2) from beginning. (c) Projection in the  $x_2-x_1$  plane, the same as (b).

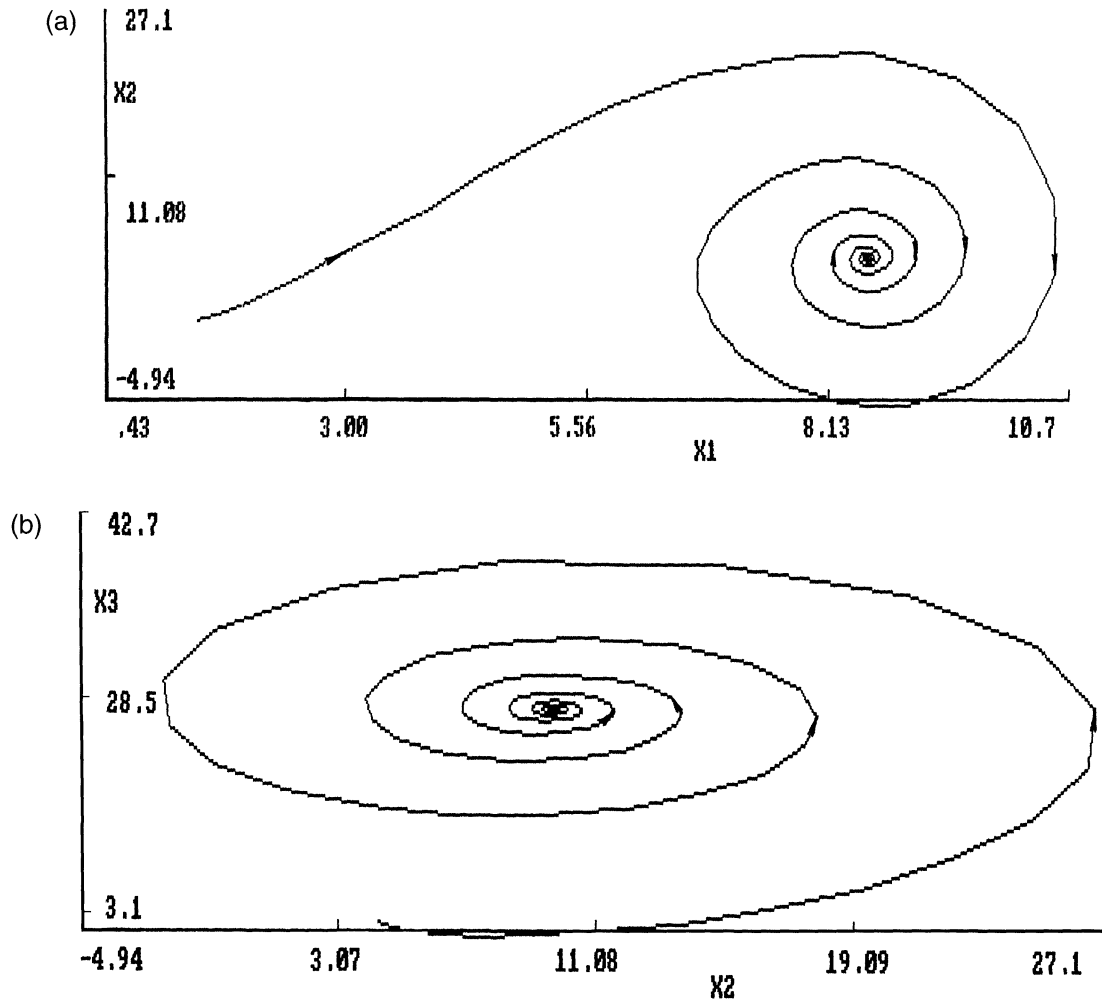


FIGURE 2 The stabilized equilibrium  $P = (8.48, 8.48, 27.00)^T$  of the Lorenz attractor, controlled by (3.3) and (3.5) in the form of (2.3) from beginning, with the same  $x(0)$  and  $\epsilon$  as in Fig. 1. (a) Projection in the  $x_2$ - $x_1$  plane. (b) Projection in the  $x_3$ - $x_2$  plane.

there is some drift distance from the target on uncertainty on the selected switching manifold. If, and only if, a controller of the form  $u = u_0 + u_{c,q}$  is used, this drift error can be eliminated (see also Fig. 4(c)), so that exact target tracking can be achieved. The Lyapunov exponents were found to be  $(-0.49, -0.58, -0.74)$  after stabilized at  $P$  or  $Q$  in this simulation.

Figure 3 shows the other stabilization to the equilibrium  $Q$  under the same control law as the one used in Fig. 2, but with a different initial condition  $x(0) = (-15, -15, 25)^T$ . This evidence supports

another important theoretical point that different equilibria can be stabilized under one control law with different initial conditions.

Figure 4(a) shows the bang-bang control signal,  $\text{sgn}[\cdot]$ ; (b) is the nonlinear feedback signal,  $u$ ; and (c) indicates the convergence error versus the number of time steps corresponding to Fig. 2. We used a step size  $h = 0.0001$ , so the control time is about 10.

Furthermore, using another controller in the form of (3.6) or (3.7), numerical simulations have also shown that the two equilibria,  $P$  and  $Q$ , can be

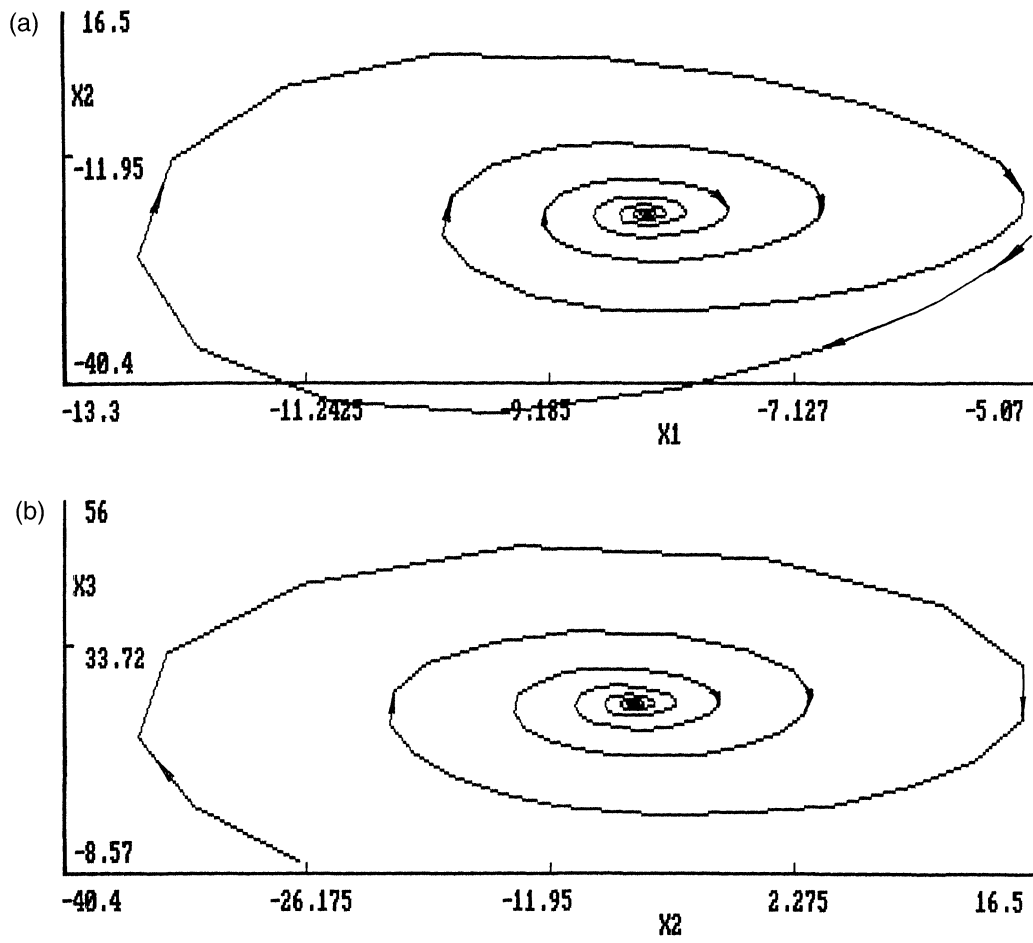


FIGURE 3 The stabilized equilibrium  $Q = (-8.485, -8.485, 27.000)^T$  of the Lorenz attractor, controlled by the same control law as in Fig. 2, but using a different initial condition  $x(0) = (-15, -15, 25)^T$ . (a) Projection in the  $x_2-x_1$  plane. (b) Projection in  $x_3-x_2$  plane.

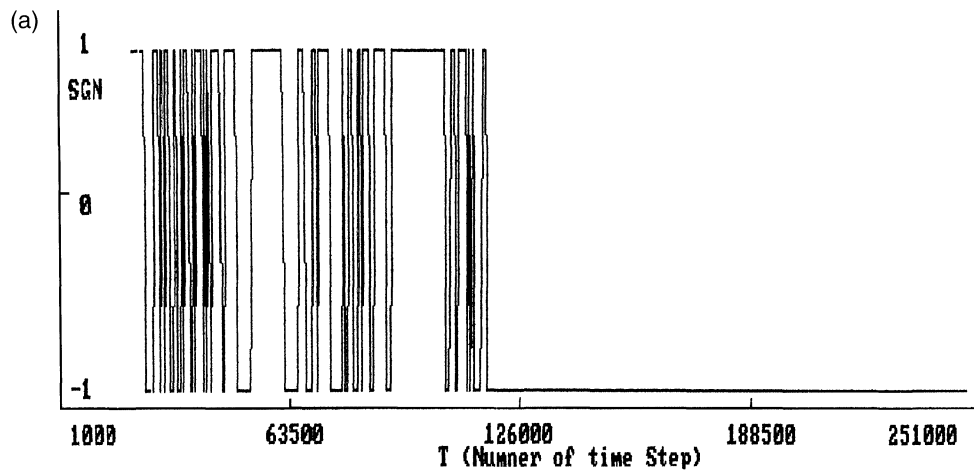


FIGURE 4(a)



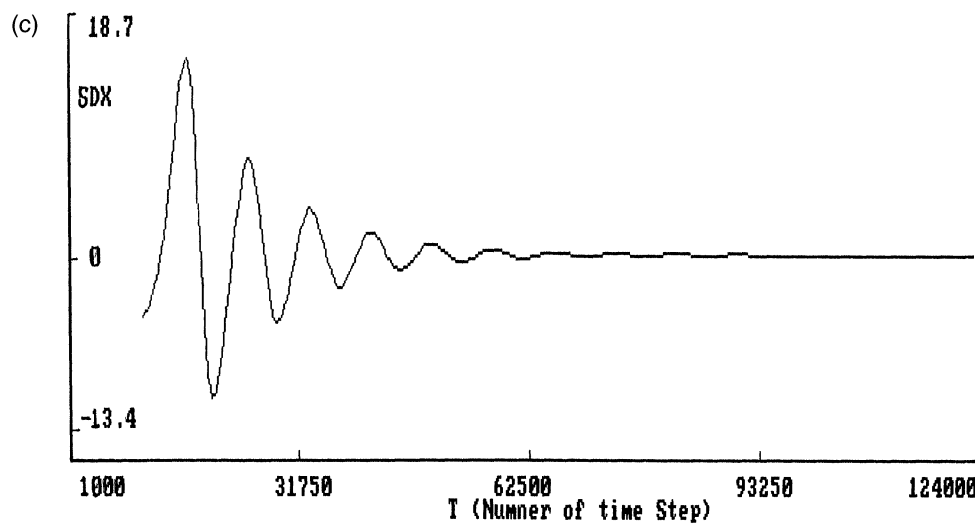
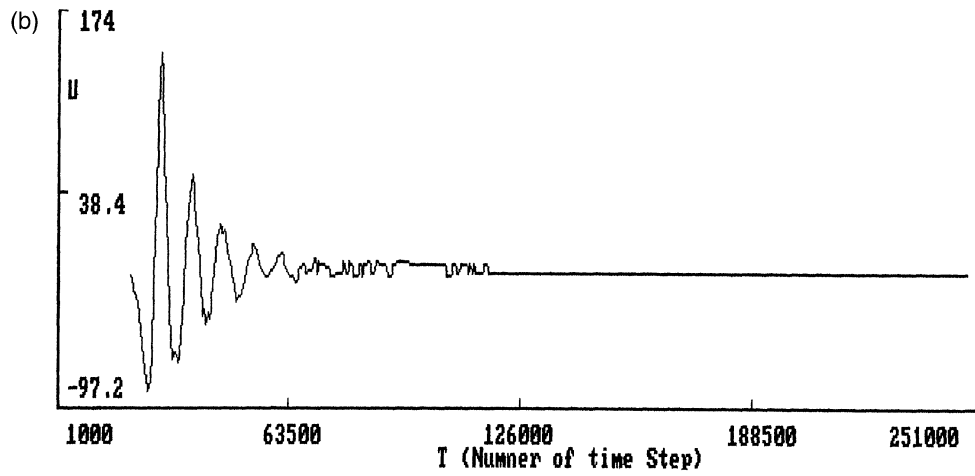


FIGURE 4(b) and (c)

FIGURE 4 (a) The bang-bang control signal,  $\text{sgn}[\cdot]$ ; (b) the nonlinear feedback signal  $u$ ; and (c) the total dynamical error SDX versus the number of time steps under the same condition as in Fig. 2. Time step size  $h = 0.0001$ .

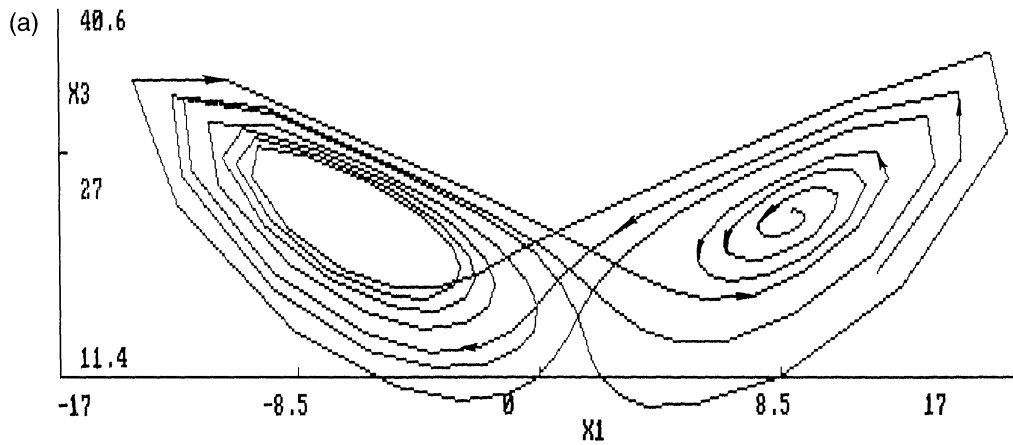


FIGURE 5(a)

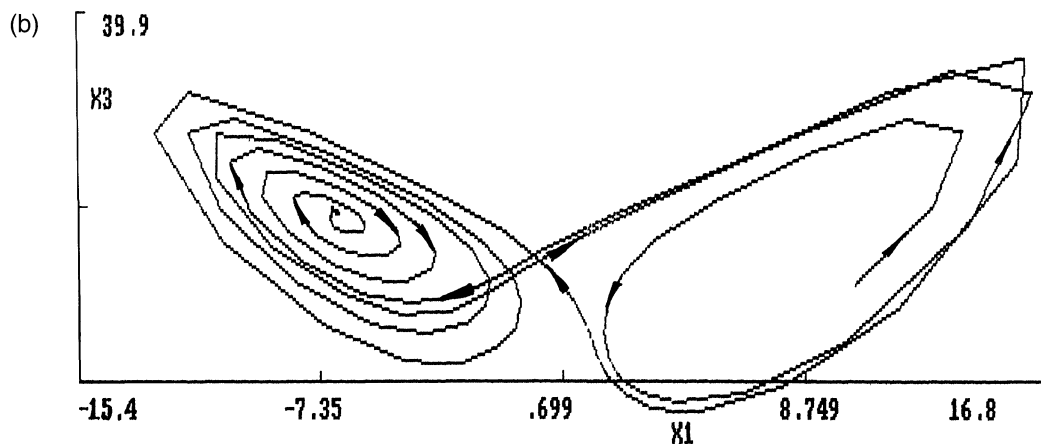


FIGURE 5(b)

FIGURE 5 Points  $P$  and  $Q$  are stabilized for the controlled Lorenz equation (2.11) by using (3.6), under the same gain  $\epsilon = 1.78$  but with two different initial conditions (a)  $x(0) = (0, -1, 0)^T$  and (b)  $x(0) = (0, 2, 7)^T$ , respectively. Controlling on from  $T = 40\,000$ . (a) Projection for controlling to  $P$  in the  $x_3$ - $x_1$  plane. (b) Projection for controlling to  $Q$  in the  $x_3$ - $x_1$  plane.

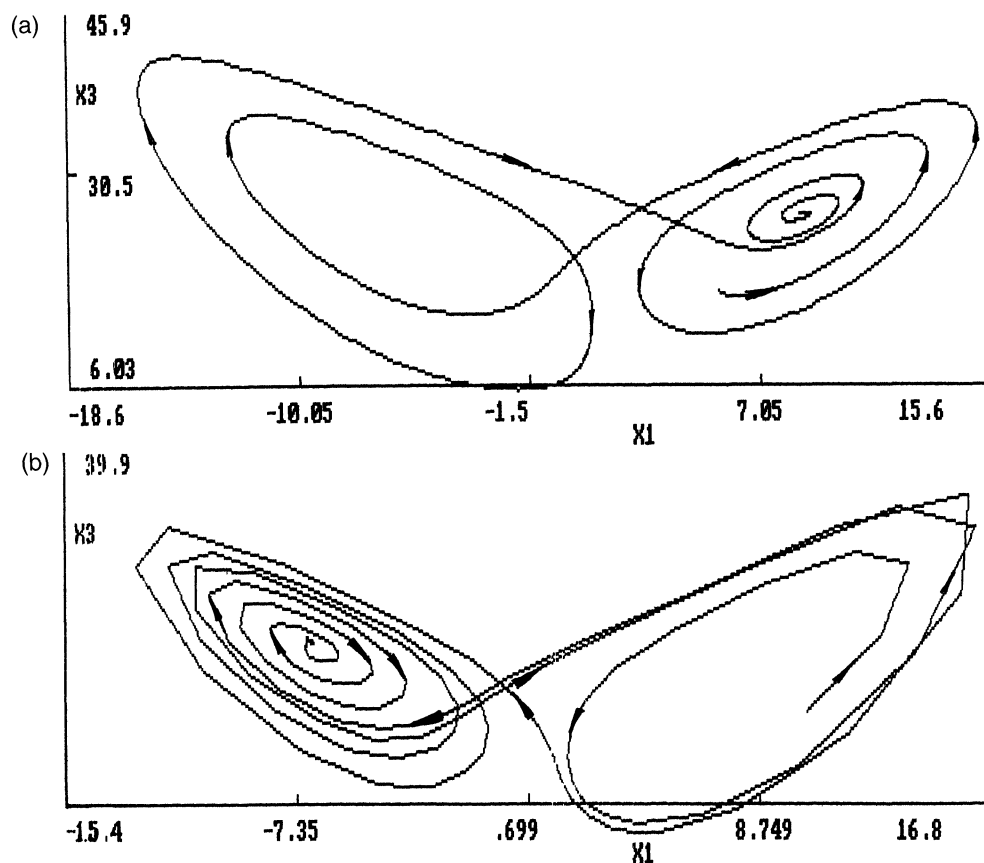


FIGURE 6 Points  $P$  and  $Q$  are stabilized for the controlled Lorenz equation (2.11) by using (3.7), under the same gain  $\epsilon = 1.78$  but with two different initial conditions (a)  $x(0) = (0, -1, 0)^T$  and (b)  $x(0) = (0, 2, 7)^T$ , respectively. Controlling on from  $T = 40\,000$ . (a) Projection for controlling to  $P$  in the  $x_3$ - $x_1$  plane. (b) Projection for controlling to  $Q$  in the  $x_3$ - $x_1$  plane.

stabilized for the controlled Lorenz system (2.11), as shown in Figs. 5 and 6, for the same feedback gain  $\epsilon = 1.78$  but with two different initial conditions  $x(0) = (0, -1, 0)^T$  and  $x(0) = (0, 2, 7)^T$ , respectively.

As can be seen from Figs. 1–6 that chaos control of the Lorenz attractor is implemented successfully by the proposed methods with very fast convergence rates. In addition, there are some important observations:

- (1) Which one of the two equilibria,  $P$  or  $Q$ , is stabilized to also depends on the feedback gain  $\epsilon$  even for the same controller under the same initial condition. For example, using (3.6) for Eq. (2.11) with  $x(0) = (0, 2, 7)^T$ , the equilibrium is stabilized to  $P$  when  $\epsilon = 1.83$ ; while it is stabilized to  $Q$  if the value of  $\epsilon$  is switched to 1.76.
- (2) There is an optimal value of the gain under which is a fastest control time to reach the point  $P$  or  $Q$ . For instance, the above  $\epsilon = 1.76$  is optimal and the control time is about 0.15.
- (3) The gain  $\epsilon$  cannot be too small or too big; otherwise it fails to control the chaos or the control time becomes too longer. In general, the range of  $\epsilon$  is observed to be in (0.5, 100) for the Lorenz system.

In summary, all the simulations results are successful, which demonstrate that the proposed two nonlinear controllers can stabilize any desired unstable equilibria and the effects of control depends on both the initial conditions and the feedback gain.

## 5 CONCLUSIONS

In this paper, chaos control is studied within the scope of stabilizing the system states to different desired unstable equilibria by using only one nonlinear feedback controller, whereas it is based on the idea of switching manifold in the spirit of variable structure control. It has been observed that to which target the state is stabilized has its own

contingency (chance), which is consistent with the certainty (or uncertainty) of chaos control, an important topic for future studies. The numerical simulation results on the Lorenz system have demonstrated the theoretical analysis and the effectiveness of the control methods. Potential applications of the proposed chaos control methods include stabilization of different equilibria in condensed matter and chemical reactions, among others.

## Acknowledgement

This work was supported by the National Natural Science Foundation of China, the National Climbing Project of China, a grant from the National Nuclear Industry Science Foundation of China, and the China National Project of Science and Technology for Returned Student in Non-Education System.

## References

- [1] W.L. Ditto, M.L. Spano and J.F. Lindner, *Physica D*, **86** (1995) 198.
- [2] E. Ott, T. Sauer and J.A. Yorke, *Coping with Chaos*, John Wiley and Sons, Int. New York, 1994.
- [3] G. Chen and X. Dong, *IEEE Trans. Circuits and Systems*, **40** (1993) 591.
- [4] G. Chen and X. Dong, *J. Circuits, Systems, and Computer*, **3** (1993) 139.
- [5] G. Chen and X. Dong, *Inter. J. Bifur. and Chaos*, **3** (1993) 1363.
- [6] G. Chen, *Chaos, Solitons and Fractal*, **8** (1997) 1461.
- [7] J. Guckenheimer and P. Holmes, *Nonlinear Oscillations, Dynamical Systems, and Bifurcations of Vector Fields*, Springer-Verlag, New York, 1983.
- [8] Proceedings of Workshop on Nonlinear Control and Control chaos, Trieste, Italy, June 17–28, 1996; Some references therein, such as: H. Nijmeijer, H. Troger, and so on.
- [9] H. Nijmeijer and A.J. van der Schaft, *Nonlinear Dynamical Control Systems*, Springer-Verlag, New York, 1991.
- [10] V. Petrov and K. Showalter, *Phys. Rev. Lett.*, **76** (1996) 3312.
- [11] M.K. Ali and J.-Q. Fang, *Phys. Rev. E*, **55** (1997) 5285; *Discrete Dynamics in Nature and Society*, **1** (1997) 197.
- [12] J.-Q. Fang and M.K. Ali, *Chin. Phys. Lett.*, **4** (1997) 823; *Nuclear Science and Techniques* **8** (1997) 129, 193.
- [13] D.W. Russell, Using the boxes methodology as a possible stabilizer of Lorenz chaos. *Artificial Intelligence—Sowing Seeds of the Future*, edited by C. Zhang, J. Debenham and D. Lukose, Singapore, World Scientific, pp. 338–345.
- [14] X. Yu, *Int. J. of Syst. Sciences*, **27** (1997) 355.
- [15] T.-L. Liao and N.-S. Huang, *Phys. Lett. A*, **29** (1997) 262.